# Deep learning based liver cancer detection using watershed transform and Gaussian mixture model techniques

**Amita Das[a], U. Rajendra Acharya[b,c,d] Soumya S. Panda[e], Sukanta Sabut[f*]**

[a]Dept. of Electronics & Communication Engineering, SOA Deemed to be University, India

[b]Dept. of Electronics and Computer Engineering, Ngee Ann Polytechnic, Singapore

[c]Dept. of Biomedical Engineering, School of Science & Technology, Singapore University of Social Science, Singapore

[d]School of Medicine, Faculty of Health and Medical Sciences, Taylor's University, 47500 Subang Jaya, Malaysia

[e]Dept. of Surgical Oncology, IMS & SUM Hospital, SOA Deemed to be University, India

[f]School of Electronics Engineering, KIIT Deemed to be University, India

*Corresponding author: sukanta.sabatfet@kiit.ac.in

## Abstract

*Objectives:* Liver cancer is one of the leading cause of death in all over the world. Detecting the cancer tissue manually is a difficult task and time consuming. Hence, a computer-aided diagnosis (CAD) is used in decision making process for accurate detection for appropriate therapy. Therefore the main objective of this work is to detect the liver cancer accurately using automated method.

*Methods:* In this work, we have proposed a new system called as watershed Gaussian based deep learning (WGDL) technique for effective delineate the cancer lesion in computed tomography (CT) images of the liver. A total of 225 images were used in this work to develop the proposed model. Initially, the liver was separated using marker controlled watershed segmentation process and finally the cancer affected lesion was segmented using the Gaussian mixture model (GMM) algorithm. After tumor segmentation, various texture features were extracted from the segmented region. These segmented features were fed to deep neural network (DNN) classifier for automated classification of three types of liver cancer i.e. hemangioma (HEM), hepatocellular carcinoma (HCC) and metastatic carcinoma (MET).

*Results:* We have achieved a classification accuracy of 99.38%, Jaccard index of 98.18%, at 200 epochs using DNN classifier with a negligible validation loss of 0.062 during the classification process. Conclusions: Our developed system is ready to be tested with huge database and can aid the radiogists in detecting the liver cancer using CT images.

*Keywords:* Liver cancer, CT scan, watershed transform, Gaussian mixture model, DNN model.

## 1. Introduction

Liver cancer is the common cause of death worldwide. The cancerous tissue can be identified accurately using computed tomography (CT) images [1]. In the image processing approach, the computer-aided diagnosis can be used for the classification of liver cancer in order to assist the clinician in decision making process [2]. For effective characterization of the liver cancer, image processing and artificial intelligence approaches have potential in research applications. Several algorithms in detecting liver tumor are reported that includes region-based methods, watershed transform and machine learning approach. An automated approach has been reported based on CAD system for effective classification of liver tumor using GLCM based features [3]. Huang *et al.* [4] presented a CAD based diagnosis procedure to segment and classify liver tumors within the non-enhanced CT images. In their extension work, they classified the tumor with an accuracy of 81.7%using the auto-covariance texture features [5]. Ji *et al.* [6] proposed an effective computational model for the clinical diagnosis of hepatocellular carcinoma based on a particle swarm optimization method.

A novel and effective optimized method based on instance optimization (IO) and SVM has been reported to recognize liver cancer with greater accuracy [7]. Li *et al.* [8] used an edge based distance regularized level-set evaluation method that effectively segmented the cyst, tumor, calculi, and normal liver in CT images. A multi-channel fully convolutional network (MC-FCN) model provides greater accuracy in segment liver tumors in CT images [9]. The GLCM and other feature extraction techniques are used to extract statistical features successfully in machine learning approaches [10-13]. The intensity based multi-level segmentation approach has been used successfully to detect different types of liver lesions [22]. Devi *et al.* [14] compared the classification performance between back propagation neural network and support vector machine classifier in detecting the liver tumor. The superior result was achieved in BPNN with an accuracy of 73.23%. Rajagopal *et al.* [15] obtained an accuracy of 97.83% in segmentation of liver tumor in CT images using SVM classifier. Sakr *et al.* [16] presented an automated system based on fuzzy clustering approach with a multi-SVM classifier to categories Cyst, Hem and HCC liver diseases.

In recent works, deep learning techniques using DNN have been applied successfully to solve a wide range of problems [17, 18]. In an automatic method, the convolutional neural networks (CNN) is used effectively to segment affected lesions in CT images and achieved a dice similarity coefficient of 80.06% [19]. Lu *et al.* [20] developed a deep learning algorithm with graph cut

refinement to automatically and efficiently segment the CT scans. Kaizhi *et al.* [21] reported system for classification liver diseases using deep learning. In a recent survey report, Hu *et al.* [22] discussed the deep learning approaches such as convolutional neural network, fully convolutional network, auto-encoders and deep belief networks for detection and diagnosis of cancer. In this paper, we have introduced a new automated technique based on watershed–Gaussian segmentation approach that combines the gradient of the watershed transformation, the Gaussian mixture model and deep learning classification to detect the liver tumor region. The informative features were extracted from the segmented images and classified into three type's liver cancer.

## 2. Methods

We proposed a CAD model called watershed Gaussian based deep learning (WGDL) technique, which consists of intensity based segmentation to efficiently delineate the cancer lesion in CT images of the liver. The proposed workflow for the segmentation process is presented in Figure 1. The Marker controlled watershed segmentation was used to separate the liver from other organs of the abdomen and the Gaussian mixture model (GMM) was implemented to segment the cancer tissue. The extracted statistical, textural and geometrical features were classified with the use of DNN classifier to differentiate HEM, HCC and MET types of liver tumor.

### 2.1. Dataset

A total of 225 CT images of liver cancer were collected from the imaging center of IMS and SUM Hospital, India. These are collected from 75 patients (46 male, 29 female) having hemangioma (HEM); 75 patients (55 male, 20 female) having hepatocellular carcinoma (HCC) and 75 patients (48 male, 27 female) having metastatic carcinoma (MET) types of cancer. The images were recorded using GE medical system CT scan machine having slice thickness of 0.5 mm to 1.5 mm with resolution of $512 \times 512$. The study was executed using MATLAB 2015a in a personal computer having Intel (R) core $i5 \times 64$ based processor with 8 GB RAM.
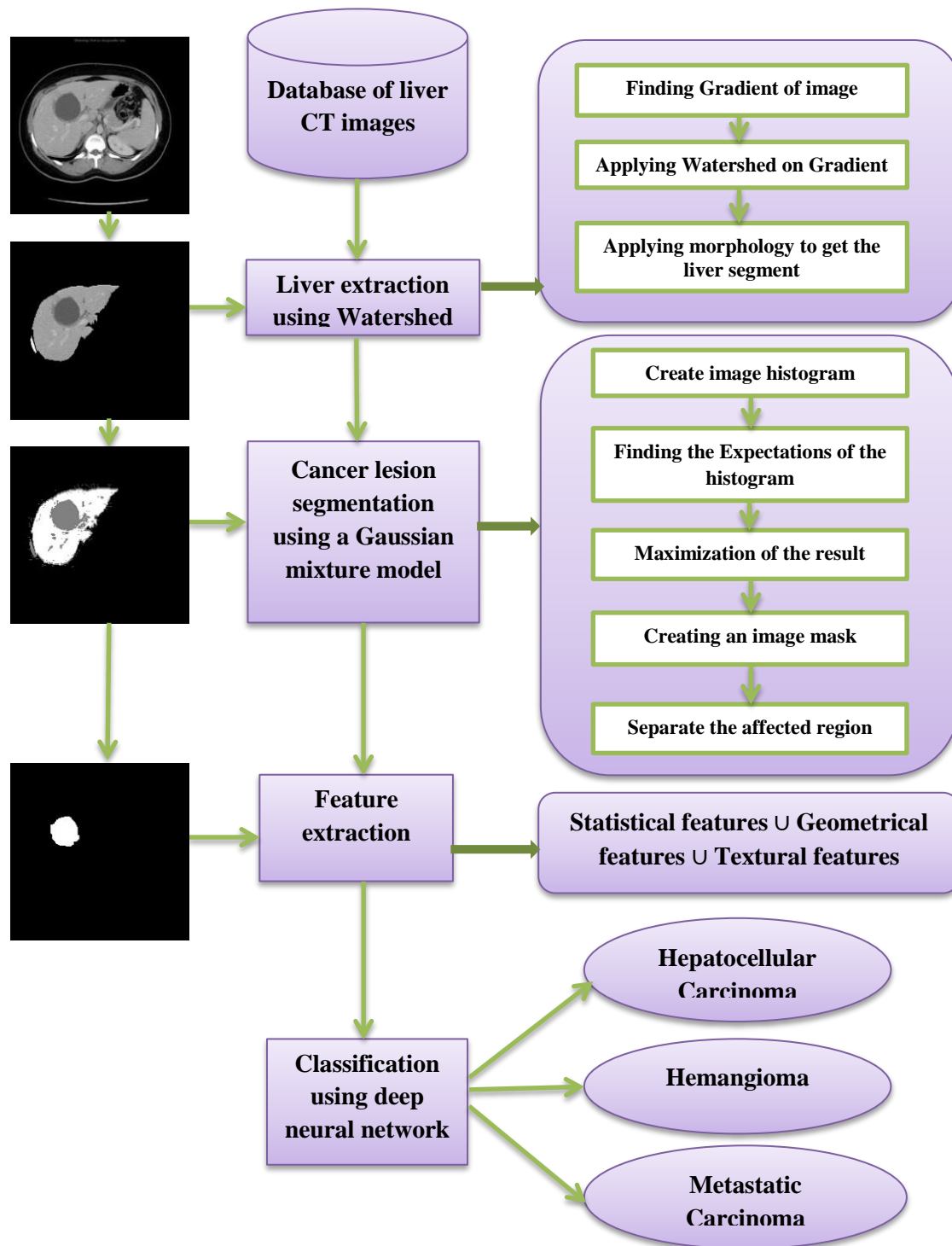
Fig. 1. The workflow of proposed CAD system.

## 2.2. Watershed transform

The Watershed transform is one of the region based segmentation algorithm based on the concept of geography [23, 24]. In this algorithm, the grayscale images are considered topographic relief, with a local minimum known as catchment basin. When the water is flooded it builds a barrier and constitutes a watershed. This approach produced total division of the image. The morphological operation is used for obtaining the image structure. This operation generally suppresses the system noise and other artifacts from the grayscale image. We applied watershed transform on the gradient image for smooth structure of the boundary.

## 2.3. Gaussian mixture model

The image is presented in terms of a matrix in which each element represents one pixel. In the Gaussian mixture model (GMM) [25], the image pixels are taken as a random variable and denoted with the variable x, where x represents a three-dimensional variable having RGB values. The probability of the image is represented by a weighted sum of Gaussian distribution by

$$f(x) = \sum_{i=1}^{k} w_i N(x|\mu_i, \sigma_i^2) \tag{5}$$

where k represents the total number of regions and the set $\{w_1, w_2, \dots, w_k\}$ defines the weights which satisfy the condition $\sum_{i=1}^{k} w_i = 1$

The term $N(x|\mu_i, \sigma_i^2)$ represents the Gaussian distribution of the ith region with the mean $\mu_i$ and standard deviation $\sigma_i$ respectively.

$$N(\mu_i, \sigma_i^2) = \frac{1}{\sigma\sqrt{2\pi}} \exp\left(\frac{-(x-\mu_i)^2}{2\sigma_i^2}\right) \tag{6}$$

To evaluate GMM, first we need to estimate the parameter of the model. The most commonly used approach to estimate the parameter $\theta$ of GMM is the maximum-likelihood estimation. The main aim of the estimation is to maximize the likelihood of GMM dataset. The expectation maximization (EM) algorithm is used for estimation.

## 2.4. Feature set

The feature extraction is a process to extract the valuable information from an image in order to classify the disease accurately [41, 42]. The statistical, geometrical and texture features were extracted from the segmented images using gray level co-occurrence matrix (GLCM) method and used for the classification. [26, 27]. The features namely contract, correlation, energy, entropy,

variance, homogeneity, sum entropy, sum variance, sum average, inverse difference moment, cluster shade, and cluster prominence are computed for an image. The statistical features includes mean, standard deviation, skewness, and kurtosis extracted from the image [28]. The geometrical features namely area, perimeter, circularity, equivalent diameter and roundness are also extracted from the extracted region. The performance was evaluated in terms of sensitivity, specificity, accuracy, dice similarity coefficient (DSC), and Jaccard index (JI) using the following equations.

$$Sensitivity = \frac{TP}{TP + FN}$$

$$Specificity = \frac{TN}{TN + FP}$$

$$Accuracy = \frac{TP + TN}{TP + TN + FP + FN}$$

$$DSC = \frac{2TP}{2TP + FP + FN}$$

where true positive (TP), false positive (FP), true negative (TN), false negative (FN).


*2.5. Deep Neural Networks*

The deep learning architecture has been applied to various classification problems and has yielded excellent classification performance [29-32]. Artificial neural networks (ANN) are the traditional computational algorithms which are inspired by the network of the biological neuron to resolve the problem of computer vision and machine learning. A deep neural network (DNN) is one type of artificial neural network with more than three layers and the outputs of the neuron are applied iteratively to their own inputs. The algorithm inherently performs the classification and directly builds the decision-making function.

In this particular work, we developed a DNN using the Keras that uses Tensorflow library and python programming language [33]. The architecture of our proposed DNN is presented in Figure 2. We have built our DNN model empirically after performing various experiments. During each experiment, we have manually constructed a DNN by modifying the subsequent parameters like the number of hidden layers, the learning steps for each hidden layer, the activation function and the total number of neurons needed to build the layer. During each manual configuration, we divided the dataset into training and testing set. The classification accuracy is evaluated over the testing set. The DNN classifier used the ReLU activation function. The output layer depends on

Softmax function relies on the cross-entropy as a cost function. The performance of the classification was evaluated using a deep neural network (DNN). Out of these 4500 features with 1500 features belonging to each of the three classes. In DNN, it is required to balance the data set otherwise the classifier will produce error function. A detailed description of training and testing sets for our proposed DNN network is reported in Table 1. The entire data set was split into 7:3 ratio and used to build the model. Table 2 describes the necessary parameters required to design the model. We have evaluated the classification accuracy of the training and testing set. The internal architecture of a DNN is presented in the Figure 2.
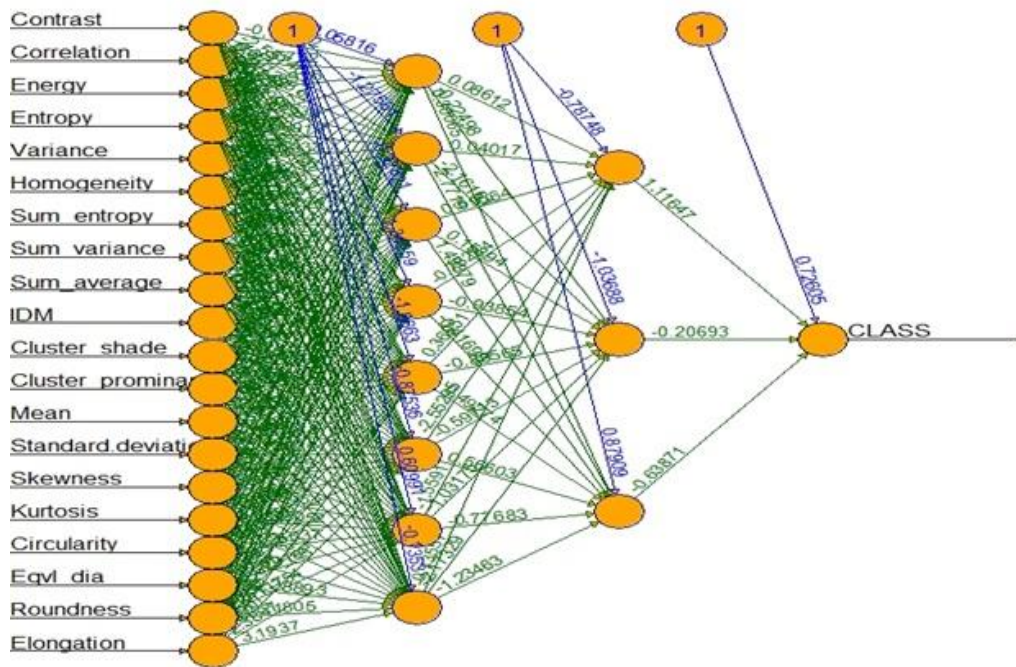


Fig. 2. The proposed architecture of DNN model.

Table 1. Details of the dataset used.

| Types of cancer | No. of patients |
|---|---|
| Hemangioma (HEM) | 75(46 male,29 female) |
| Hepatocellular Carcinoma (HCC) | 75(55 male,20 female) |
| Metastatic Carcinoma(MET) | 75(48 male,27 female) |

Table 2. Description of parameters used in our proposed DNN model.

| Model used | Sequential |
|---|---|
| Activation function(Input) | ReLU(Rectified Linear Unit) |
| Activation function(Output) | Softmax |
| Optimizer | Adam |
| Number of epochs | 200 |
| Batch_size | 32 |
| Validation_split | 0.2 |

## 3. Experimental results

The proposed method liver cancer detection was tested on 225 CT scan images having cancer lesions. The presented CAD method, consist of two stages; liver separation and cancer lesion detection. In the first stage, a guided filter is used to sharpen the edge of liver structure and watershed transform applied on gradient magnitude to separate the liver region. Finally, the liver structure is extracted from the CT image by applying regional maxima and morphological operations. In the second stage, the separated liver regions are further subjected to GMM to detach the final cancer lesion. Fig. 3 shows the output of watershed transform that used to separate the liver from the abdominal CT images. Fig. 3(a) to Fig. 3(f) presents the different stages of the separation process. This separated liver was then segmented using Gaussian mixture model to obtain the final tumor of the liver. First the histogram of the image was calculated and the mean value of each Gaussian components was estimated using the center of the image. The variance and posterior probabilities are then calculated using the mean values. The class values are initialized using K means likewise. Figure 4, 5 and 6 represents the results for the images with hemangioma, hepatocellular carcinomas and metastatic carcinomas respectively.

original image

Gradient magnitude (gradmag)

Watershed transform of gradient magnitude (Lrgb)

(a)

(b)

(c)

Regional maxima of opening-closing by reconstruction (fgm)

Modified regional maxima superimposed on original image (fgm4)
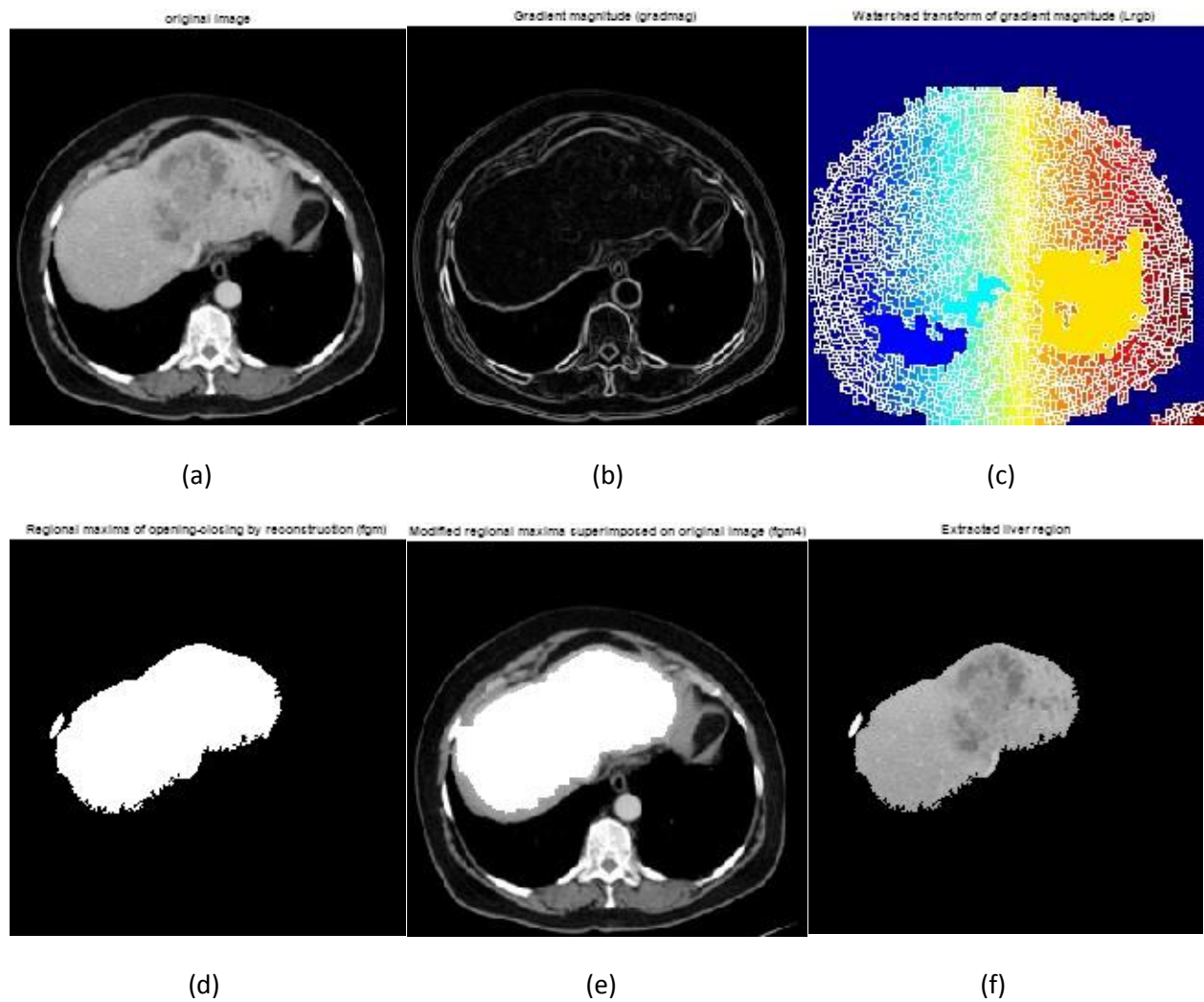
Extracted liver region

(d)

(e)

(f)

Fig. 3. Segmentation results of the watershed algorithm: (a) original image, (b) gradient magnitude image, (c) watershed transform of gradient magnitude, (d) reconstruction of regional maxima using morphological opening-closing, (e) regional maxima superimposed on the original image and (f) extracted liver region after morphological operation.
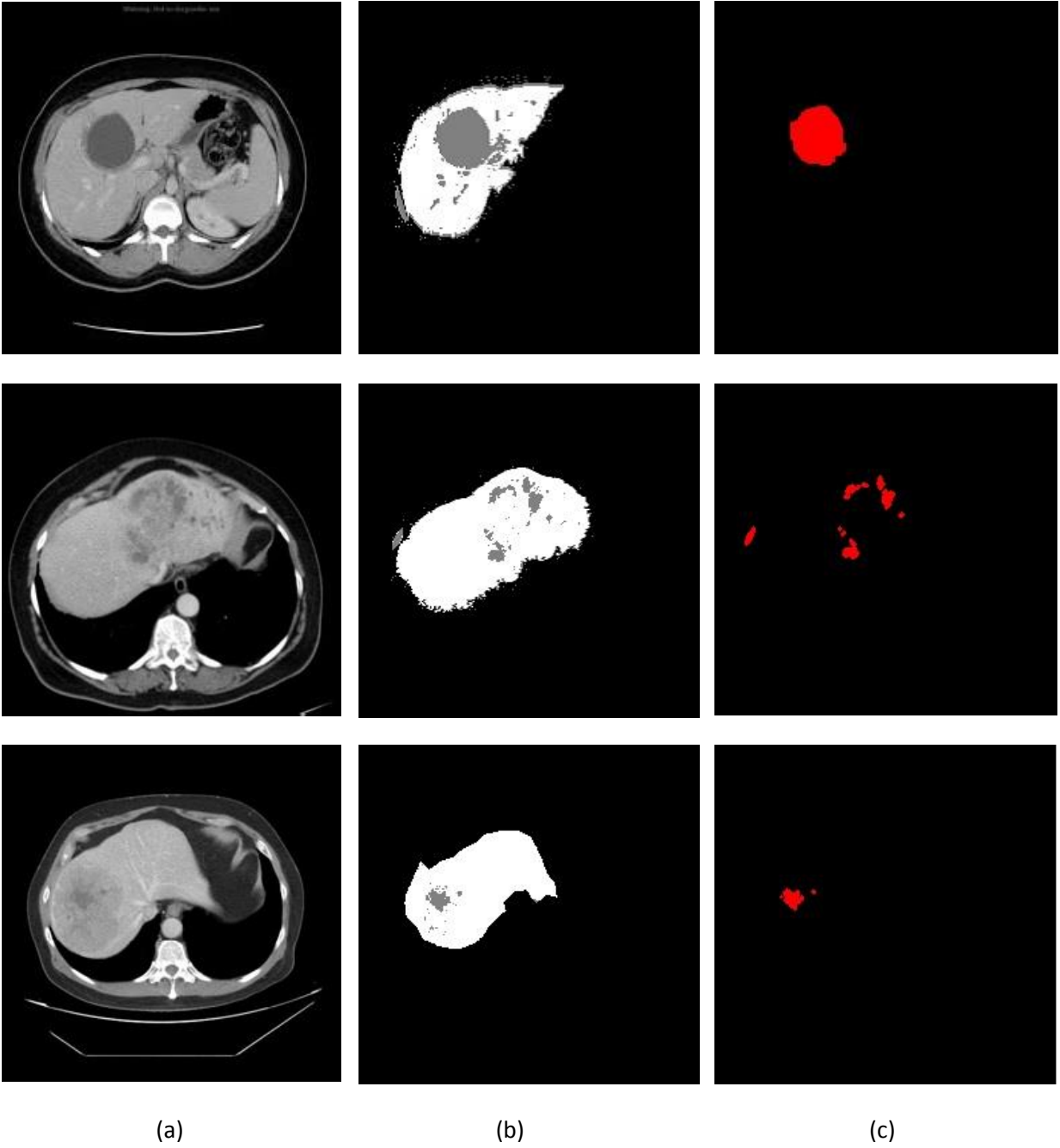
|          |          |          |
|:--------:|:--------:|:--------:|
| (a)      | (b)      | (c)      |

Fig. 4. (a) original hemangioma image: ( b) segmented cancer image after using GMM and (c) segmented ROI after applying morphological operation.
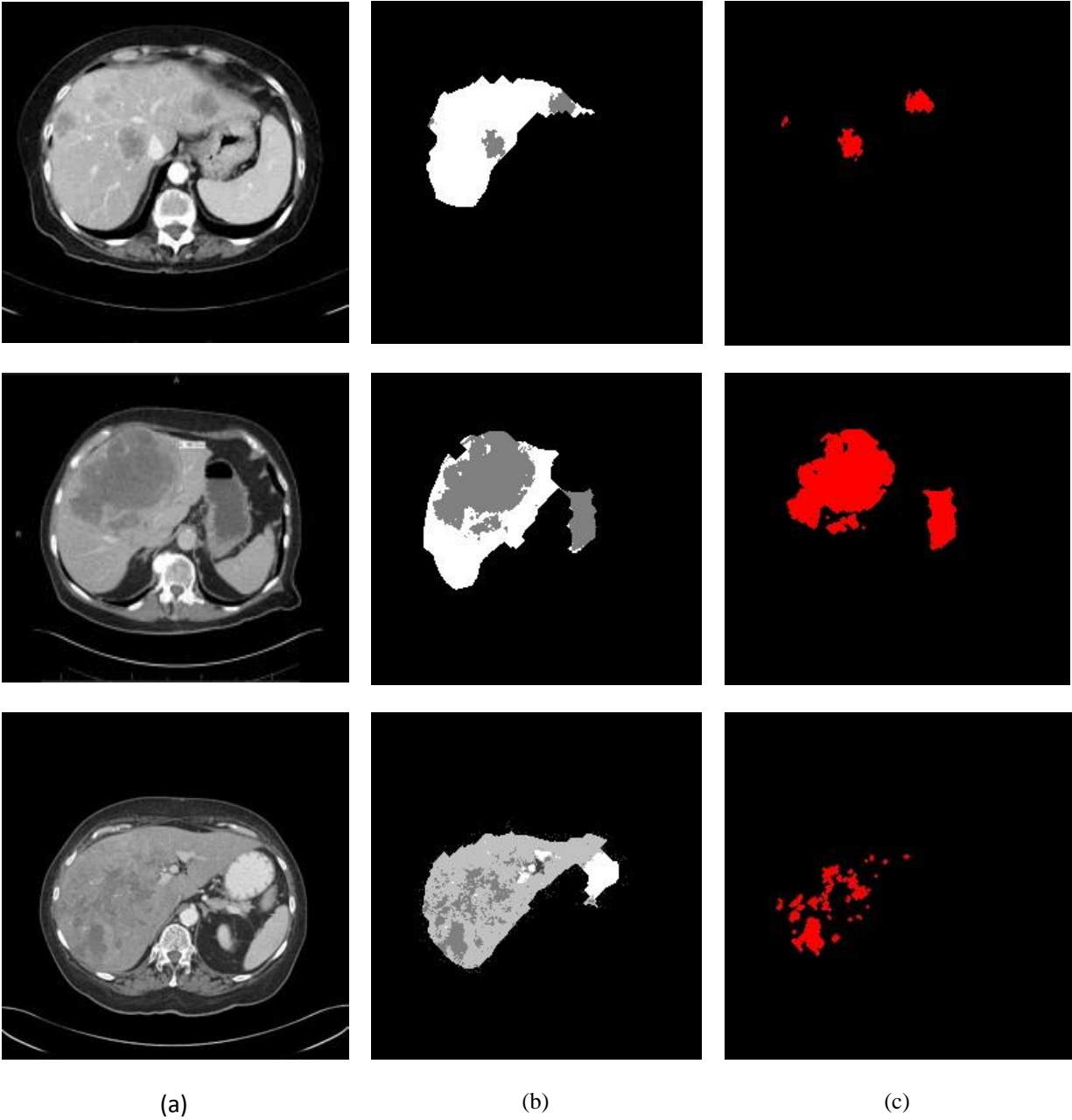
Fig. 5. (a) Original hepatocellular carcinomas image: (b) segmented cancer image after using GMM and (c) segmented ROI after applying morphological operation.
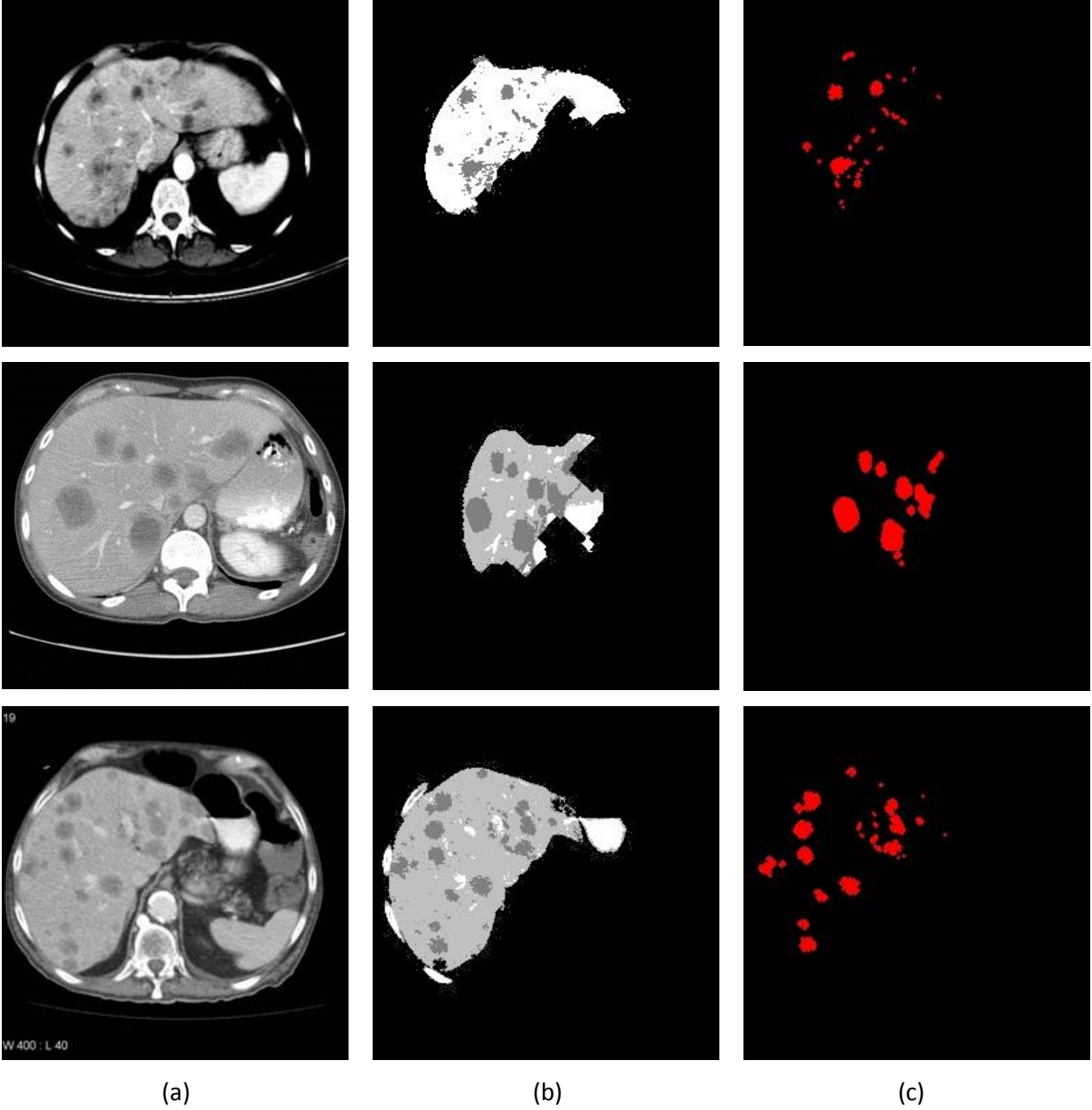
(a)                                    (b)                                    (c)

Fig. 6**.** (a) Original metastatic carcinoma image: (b) segmented cancer image after using GMM and (c) segmented ROI after applying morphological operation.

*Classification results:* The classification of hemangioma, hepatocellular carcinoma, and metastatic carcinoma was done using DNN using Tensorflow library with three-fold cross validation strategy. The dataset is spitted into 7:3 ratio, therefore 70% of the dataset are taken as training set and remaining 30% of the dataset are taken as testing set. The model was trained using 200 epochs. Table. 3 shows the confusion matrix obtain from the two datasets. The output activation function

was softmax and learning rate was set as 0.01. Figure 7 presents the training and validation error versus a number of epochs obtained in our model. As can be seen from the graph, initially the network was not performed well. That means bellow 30 epochs, the loss was more than one and accuracy is about 0.4. By increasing the number of epochs, the accuracy of training and validation increases gradually and the loss decreases. At about 200 epochs, the model achieved best accuracy of 99.38% for training dataset and loss is reduced to a nominal value of 0.062. Table 4 shows the results obtain from the training and testing sets using the formulas given bellow. We have compared the performance obtained from DNN model to few classifiers namely Naïve Bayes, multi layered perceptron (MLP), support vector machine (SVM), K-nearest neighbor (KNN), AdaBoost M1, J48 and random forest. The summary of the performance results are listed in Table 5.  It is clear from the table that the DNN model achieved an accuracy of 99.38% in training dataset.

Table 3. Confusion matrix of our proposed model after 200 epochs.

| Training set | | | | | Testing set | | | |
|---|---|---|---|---|---|---|---|---|
| Class | HEM | HCC | MET | | Class | HEM | HCC | MET |
| HEM | 54 | 0 | 0 | | HEM | 19 | 0 | 0 |
| HCC | 1 | 51 | 0 | | HCC | 1 | 24 | 0 |
| MET | 0 | 0 | 57 | | MET | 0 | 0 | 18 |

Table 4. Obtained results from proposed DNN model.

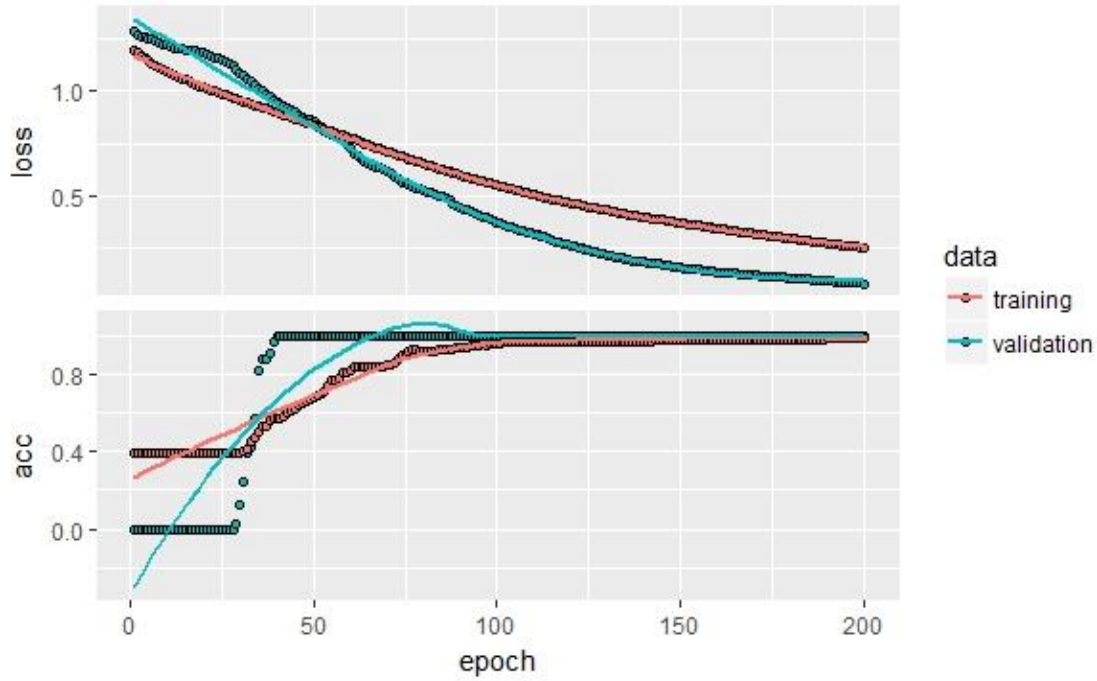| Parameters | Training set (%) | Testing set (%) |
|---|---|---|
| Accuracy | **99.39** | 98.38 |
| Sensitivity | 100 | 100 |
| Specificity | 99.09 | 97.72 |
| Jaccard index | 98.18 | 95 |
| DSC | 99.08 | 97.43 |

Fig. 7. Plot of loss and accuracy for training and validation data.

Table 5. The comparison results of different classifier.

| Classifiers | Accuracy (%) | Sensitivity (%) | Specificity (%) |
|---|---|---|---|
| Naïve Bayes | 91.94 | 89.91 | 93.65 |
| MLP | 91.65 | 89.58 | 93.08 |
| SVM | 95.17 | 94.22 | 95.76 |
| KNN | 93.87 | 92.56 | 95.31 |
| AdaBoost M1 | 90.72 | 87.97 | 92.47 |
| J48 | 95.98 | 95.11 | 96.58 |
| Random forest | 94.86 | 93.88 | 95.38 |
| **DNN model** | **98.38** | **100** | **99.09** |

## 4. Discussion

Manual segmentation of cancerous tissue from the CT image is time-consuming and operator dependent. Therefore computer-aided methods are used to detect the abnormal tissues for in automatic diagnosis of the liver cancer. In this study, we have proposed an automated watershed-Gaussian based deep learning (WGDL) technique to detect and identify three different types of

liver cancer in CT images. The main objective of this study was to implement the strength of two integrated methods i.e. marker controlled Watershed transform and Gaussian mixture model for accurate delineation of cancerous lesion. The informative features were extracted from the segmented images and used in the deep learning classifier to differentiate between Hemangioma, Hepatocellular carcinoma and Metastatic carcinoma cells. The presented CAD method, consist of two stages; liver separation using watershed transform and detection of cancer with GMM model. Few recent articles highlighted the use of different methods in the process of tumor segmentation and classification.

The proposed watershed and GMM based algorithms influences the performance of the method by providing an efficient segmentation of cancerous lesion. The performance of the method was evaluated using extracted features and classified with different classifiers. From the result table, it can be observed that the deep neural network based classifier provides superior classification accuracy 98.38% and sensitivity of 100% with negligible model loss of only 0.0620. The obtained results of our method is compared with few published articles which are represented in Table 6. It can be seen from the table that, we have achieved the best classification results in all the measured parameters. Hence the deep neural model is the best choice to detect the liver tumors in automated process. The main advantages of this method is that the automated method reduces the human error and can be implemented with mass screening process. The deep neural network model has been implemented in classification process which has improved the classification accuracy with less error. The disadvantages is that the total number of CT images used in this work is less and the calculation of the computational complexity of the work. The process can be improved further with considering the 3D visualization of volumetric image in detecting tumors, which will be done as the future scope of the work.

Table 4. Summary of the work reported on automated detection of liver cancer in CT images.

| Authors | Classes | Classifiers | Accuracy (%) |
|---|---|---|---|
| Gletsos *et al.* [34] | Normal Hepatic cyst, Hemangioma | Neural network classifier(NN) | 97 |
| Chang *et al.* [15] | Benign, Malignant | Binary logistic regression analysis | 81.69 |
| Ghamisi *et al.* [36] | Liver tumor | CNN model | 80.06 |

| Ciecholewski *et al.* [37] | hemangiomas and hepatomas | Binary filtration | 78.3 |
|---|---|---|---|
| Sethi *et al.* [38] | Tumor, cyst calculi, normal liver | Genetic Algorithm, SVM, ANN | 95.1 |
| Li *et al.* [39] | Liver tumor | CNN model | 80.06 |
| Kumar *et al.* [40] | Hepatocellular, Hemangioma | Probabilistic neural network (PNN) | 96.7 |
| **Proposed** | **HCC, hemangioma, metastatic carcinoma** | **Deep neural network classifier** | **99.39** |

## 5. Conclusion

In this paper, we have introduced a new methodology for the automatic detection of liver tumors in CT images. This method is dependent on marker-controlled watershed transformation and Gaussian mixture model to detect the cancer lesion reliably. The proposed algorithm is validated on real-time clinical dataset obtained from different patients in clinical set-up. The main advantage of this automated detection process is that it produced best accuracy of 99.38% with negligible validation loss using deep neural network classifier. The implementation of DNN model in detection process is of its first kind of application in detection of liver tumor. Hence, the proposed method is an effective way to detect the cancer region from liver CT images that will be helpful in clinical diagnosis and decision-making process for early diagnosis of the symptoms. The calculation of the volumetric size of the lesion is the main limitation of the work, which can be formed by making 3-D mesh structure from different slice of the images.

## References

1. Bartolozzi, C., Ciatti, S., & Lucarelli, E. (1981). Ultrasound and computer tomography in the evaluation of focal liver disease. Acta Radiol., 22, 545–548.
2. Kononenk, I. (2001). Machine learning for medical diagnosis. History, state of the art and perspective. Artif Intell Med., 23, 89–109.
3. Chen, E., Chung, P., Chen, C., Tsai, H., & Chang, I. (1998). An automatic diagnostic system for CT liver image classification. IEEE Trans Biomed Eng., 45,783–94.
4. Huang, Y., Chen, J. & Shen, W. (2004). Computer-aided diagnosis of liver tumors in non-enhanced CT images. J Med Phys., 9,141–50.

5. Huang, Y., Chen, J. & Shen, W. (2006). Diagnosis of hepatic tumors with texture analysis in non-enhanced computed tomography images. Acad Radiol., 13, 713–20.

6. Ji, Z. & Wang, B. (2014). Identifying potential clinical syndromes of hepatocellular carcinoma using PSO-based hierarchical feature selection algorithm. Biomed Res Int., 1-12.

7. Jiang, H., Zheng, R., Yi, D. & Zhao, D. (2013). A novel multi-instance learning approach for liver cancer recognition on abdominal CT images based on CPSO-SVM and IO. Comput Math Methods Med., 1-10.

8. Li, C., Xu, C., Gui, C. & Fox, M. (2010). Distance regularized level set evolution and its application to image segmentation. IEEE Trans Image Process, 19, 3243–54.

9. Sun, C., Guo, S., Zhang, H., Li, J., Chen, M., Ma, S., Jin, L., Liu, X., Li, X. & Qian, X. (2017). Automatic segmentation of liver tumors from multiphase contrast-enhanced CT images based on FCNs. Artif Intell Med., 83, 58-66.

10. Haralick, R., Shanmugam, K. & Dinstein, I. (1927). Textural features for image classification. IEEE Trans Syst Man Cybern., 3,610–21.

11. Newell, D., Nie, K., Chen, J.H., Hsu, C.C, Yu, H.J, Nalcioglu, O. & Su, M.Y. (2010). Selection of diagnostic features on breast MRI to differentiate between malignant and benign lesions using computer-aided diagnosis: differences in lesions presenting as mass and non-mass-like enhancement. Eur. Radiol., 20, 771–781.

12. Nie, K., Chen, J.H. , Yu, H.J., Chu, Y., Nalcioglu, O. & Su, M.Y. (2008). Quantitative analysis of lesion morphology and texture features for diagnostic prediction in breast MRI. Acad. Radiol., 15, 1513–1525.

13. Moon, W.K., Shen, Y.W., Huang, C.S., Chiang, L.R. & Chang, R.F. (2011). Computer-aided diagnosis for the classification of breast masses in automated whole breast ultrasound images. Ultrasound Med. Biol., 37, 539-548.

14. Devi, P. & Dabas, P. (2015). Liver tumor detection using artificial neural networks for medical images. International Journal for Innovative Research in Science and Technology, 2, 34-38.

15. Rajagopal, R. & Subbaiah, P. (2014). Computer aided detection of liver tumor using SVM classifier. Int. J. Advanced Research in Electrical, Electronics and Instrumentation Engineering, 3, 10170-10177.

16. Sakr, A.A., Fares, M.E. & Ramadan, M., (2014). Automated Focal Liver Lesion Staging Classification based on Haralick Texture Features and Multi-SVM. International Journal of Computer Applications, 92, 17-25.

17. Sun, C., Guo, S., Zhang, H., Li, J., Chen, M., Ma, S., Jin, L., Liu, X., Xueyan, Li. & Qian, X. (2017). Automatic segmentation of liver tumors from multiphase contrast-enhanced CT images based on FCNs. Artificial Intelligence in Medicine, 83, 58-66.

18. Cohen, A.B., Klang, E., Kerpel, A., Konen, E., Amitai, M.M. & Greenspan, H. (2018). Fully convolutional network and sparsity based dictionary learning for liver lesion detection in CT examinations. Neurocomputing, 275, 1585-1594.

19. Li, C., Wang, X., Fulham, S.E.M., Yin, Y., Chen, J. & Feng, D.D. (2013). A likelihood and local constraint level set model for liver tumor segmentation from CT volumes. IEEE Transactions on Biomedical Engineering, 60, 2967-2977.

20. Lu, F., Wu, F., Hu, P., Peng, Z. & Kong, D. (2017). Automatic 3D liver location and segmentation via convolutional neural network and graph cut. Int. J. Comput. Assist. Radiol. Surg., 12, 171-182.

21. Kaizhi, W., Chen, X. & Ding, M. (2014). Deep learning based classification of focal liver lesions with contrast-enhanced ultrasound. Optik, 125, 4057-4063.

22. Hu, Z., Tang, J., Wang, Z., Zhang, K., Zhang, L. & Sun, Q. (2018). Deep learning for image based cancer detection and diagnosis-A survey. Pattern Recognition, 83,134-149.

23. Masoumi, H., Behrad, A., Pourmina, M.A. & Roosta, A. (2012). Automatic liver segmentation in MRI images using an iterative watershed algorithm and artificial neural network. Biomedical Signal Processing and Control, 7, 429-437.

24. Chattaraj, A., Das, A. & Bhattacharya, M. (2017). Mammographic image segmentation by marker controlled watershed algorithm. IEEE International Conference on Bioinformatics and Biomedicine (BIBM), 1000-1003.

25. Kermani, S., Samadzadehaghdam, N. & EtehadTavakol, M. (2015). Automatic color segmentation of breast infrared images using a Gaussian Mixture Model. Optik, 126, 3288–3294.

26. Subudhi, A., Jena, S. & Sabut, S. (2018). Delineation of the ischemic stroke lesion based on watershed and relative fuzzy connectedness in brain MRI. Med Biol. Eng. Comput., 56(5), 795-807.

27. Ge, Q., Xiao, L., Zhang, J. & Wei, Z.H. (2012). An improved region-based model with local statistical features for image segmentation. Pattern Recognition, 45(4), 1578-1590.

28. Du-Buf J.M, Kardan H, Spann M, Texture feature performance for image segmentation. Pattern Recognition, 1990; 23(3-4): 291-309.

29. Sannino, G. & Pietro, G.D. (2018). A deep learning approach for ECG-based heartbeat classification for arrhythmia detection. Future Generation Computer Systems, 86, 446-455.

30. Cao, C., Liu, F., Tan, H., Song, D., Shu, W., Li, W., Zhou, Y., Bo, X. & Xie, Z. (2018). Deep Learning and Its Applications in Biomedicine. Genomics Proteomics Bioinformatics, 16, 17–32.

31. Mathews, S.M., Kambhamettu, C. & Barner, K.E. (2018). A novel application of deep learning for single-lead ECG classification. Computers in Biology and Medicine, 99, 53-62.

32. Ben-Cohen, A., Klang, E., Kerpel, A., Konen, E., Amitai, M.M. & Greenspan, H.(2018). Fully convolutional network and sparsity based dictionary learning for liver lesion detection in CT examinations. Neurocomputing, 275, 1585-1594.

33. Wu, K., Chen, X. & Ding, M. (2014). Deep learning based classification of focal liver lesion with contrast enhanced ultrasound. Optik, 125,4057-4063.

34. Gletsos, M., Mougiakakou, G., Matsopoulos, K., Nikita, S., Nikita, A. & Kelekis, D. (2003). A computer-aided diagnostic system to characterize CT focal liver lesions design and optimization of a neural network classifier. IEEE Trans. Inf. Technol Biomed, 7,153-62.

35. Chang, C.C., Chen, H.H., Chang, Y.C., Yang, M.Y., Lo, C.M., Ko, W.C., Lee, Y.F., Liu, K.L. & Chang, R.F. (2017). Computer-aided diagnosis of liver tumors on computed tomography images. Computer Methods and Programs in Biomedicine, 145, 45-51.

36. Ghamisi, P., Couceiro, M.S., Benediktsson, J.A. & Ferreira, N.F. (2012). An efficient method for segmentation of images based on fractional calculus and natural selection. Expert Systems with Applications, 39(16), 12407-12417.

37. Ciecholewski, M. & Ogiela, M.R. (2007). Automatic segmentation of neoplastic hepatic disease symptoms in CT images. Int. Conf. on Modeling Decisions for Artificial Intelligence, Kitakyushu, Japan, 414-421.

38. Sethi, G. & Saini, B.S. (2016). Computer aided diagnosis system for abdomen diseases in computed tomography images. Biocybernetics and Biomedical Engineering, 36, 42 – 55.

39. Li, W., Jia, F. & Hu, Q. (2015). Automatic segmentation of liver tumor in CT images with deep convolutional neural networks. J. Comp. Commun., 3(11), 146–51.

40. Kumar, S., Moni, R. & Rajeesh, J. (2013). An automatic computer-aided diagnosis system for liver tumors on computed tomography images. Comput Electr Eng, 39, 1516–26.

41. Subudhi, A., Jena, S. & Sabut, S. (2018). Delineation of the ischemic stroke lesion based on watershed and relative fuzzy connectedness in brain MRI. Med Biol Eng Comput., 56(5), 795-807.

42. Koh, J.W., Hagiwara, Y., Oh, S.L., Tan, J.H., Ciaccio, E.J., Green, P.H., Lewis, S.K. & Acharya, U.R. (2019). Automated diagnosis of celiac disease using DWT and nonlinear features with video capsule endoscopy images. Future Generation Computer Systems, 90, 86-93.